HEAVY QUARK THERMODYNAMICS WITH ANISOTROPIC LATTICES*

Jon-Ivar Skullerud [a], Rachel Horohan D'Arcy [a]
Gert Aarts [b], Chris Allton [b], M. Naeem Anwar [b]
Timothy J. Burns [b], Ben Page [b], Ryan Bignell [c]
Sinéad M. Ryan [c], Benjamin Jäger [d], Seyong Kim [e]
Maria Paola Lombardo [f], Alexander Rothkopf [g]
Antonio Smecca [h,b]

[a]Department of Physics, National University of Ireland Maynooth
Maynooth, County Kildare, Ireland
[b]Centre for Quantum Fields and Gravity, Department of Physics
Swansea University, Swansea, SA2 8PP, United Kingdom
[c]School of Mathematics and Hamilton Mathematics Institute
Trinity College Dublin, Dublin, Ireland
[d]Quantum Field Theory Center & Danish IAS
Department of Mathematics and Computer Science
University of Southern Denmark, 5230 Odense M, Denmark
[e]Department of Physics, Sejong University, Seoul 05006, Korea
[f]INFN, Sezione di Firenze, 50019 Sesto Fiorentino (FI), Italy
[g]Department of Physics, Korea University, Seoul 02841, Korea
[h]INFN, Sezione di Roma Tre, Via della Vasca Navale 84, 00146 Rome, Italy

Received 17 April 2026, accepted 28 April 2026,
published online 10 July 2026

We present recent results from the Fastsum Collaboration, using anisotropic lattice QCD to study spectral properties of heavy quarkonia and open heavy flavour systems at high temperature. For heavy quarkonium, our results using a number of different methods suggest a small but significant and robust negative mass shift as well as an increasing thermal width. We present the first lattice results for masses and spectral functions of B mesons at high temperature, and preliminary results for a high-precision calculation of the static quark potential.

DOI:10.5506/APhysPolBSupp.19.4-A28

1. Introduction

Heavy quarks are among the most prominent probes of heavy-ion collisions [1]: due to their large mass, they are predominantly created in the initial hard collisions and subsequently experience the full space-time evolution

* Presented at the Excited QCD 2026 Workshop, Granada, Spain, 8–14 January, 2026.

of the plasma. Their interactions with the hot medium encode key information about transport properties such as diffusion coefficients and energy loss mechanisms. Furthermore, the partial thermalization of heavy quarks and their participation in collective flow provide insight into the degree of coupling within the QGP.

The properties of the quarks and their bound states in the medium are encoded in spectral functions which are related to the Euclidean correlators that can be computed on the lattice by a (generalised) Laplace transform. Inverting this relation to obtain the spectral function given the Euclidean correlator is a well-known ill-posed problem. This problem may be ameliorated by using anisotropic lattices with a finer resolution in (imaginary) time than in the spatial directions. The Fastsum Collaboration has pioneered the use of anisotropic lattices for this purpose. In these proceedings, we will present recent results on three topics related to heavy quarks in the medium: thermal mass shift and width of bottomonium, open-beauty mesons, and the real-time static quark potential.

2. Lattice setup

Our simulations are carried out using anisotropic lattices with an $\mathcal{O}(a^2)$ improved gauge action and an $\mathcal{O}(a)$ improved Wilson fermion action with stout smearing, following the parameter tuning and ensembles generated by the Hadron Spectrum Collaboration [2, 3]. The results presented here were produced using the Gen2 and Gen2L ensembles, which have $N_f = 2+1$ active quark flavours with $m_\pi \approx 380$ and 240 MeV, respectively, and an approximately physical strange quark. The spatial lattice spacing is $a_\mathrm{s} = 0.1205(8)$ fm (Gen2) and 0.1121(3) fm (Gen2L), and the anisotropy $\xi = a_\mathrm{s}/a_\tau = 3.45$. The temperature is given by $T = (a_\tau N_\tau)^{-1}$ and is varied by changing the number of sites N_τ in the temporal direction, see Table 1. For more details about the ensembles, see Refs. [4–6] and references therein.

Table 1. Lattice temporal extents N_τ and temperatures T used in this study, in units of MeV and of the chiral transition temperature T_c.

	N_τ	128	64	56	48	40	36	32	28	24	20	16
Gen2	T [MeV]	44			117	141	156	176	201	235	281	352
	T/T_c	0.24			0.65	0.78	0.86	0.97	1.11	1.3	1.6	1.9
Gen2L	T [MeV]	47	95	109	127	152	169	190	217	253	304	380
	T/T_c	0.28	0.57	0.65	0.76	0.91	1.01	1.14	1.3	1.5	1.8	2.3

3. Thermal mass and width of quarkonium

Using our Gen2L ensembles, we have compared a number of different methods for determining the thermal mass shift and width of heavy quarkonia. We have simulated the b quarks using an NRQCD action including $\mathcal{O}(v^4)$ and leading spin-dependent corrections, with mean-field improved tree-level coefficients [7]. We have employed direct correlator analysis using time-derivative moments [8] and a generalised eigenvalue problem (GEVP) analysis [9], linear methods: Tikhonov, Backus–Gilbert and Hansen–Lupo–Tantalo (HLT) [10], and Bayesian methods: maximum entropy (MEM) and the BR method [11]. Further details are given in Ref. [12].

Figure 1 shows the thermal mass shift and width of the $\Upsilon(1S)$ from the different methods. Where possible, these have been determined by applying the same analysis to the correlators from our coldest lattice, $N_\tau = 128$ (which we term $T = 0$), with temporal extent truncated to match that of the corresponding thermal correlator. The resulting mass and width have been subtracted from the thermal result to give the mass shifts and widths shown. Where this analysis has not yet been performed, the values obtained from the $T = 0$ ensemble with the full temporal extent have been subtracted.

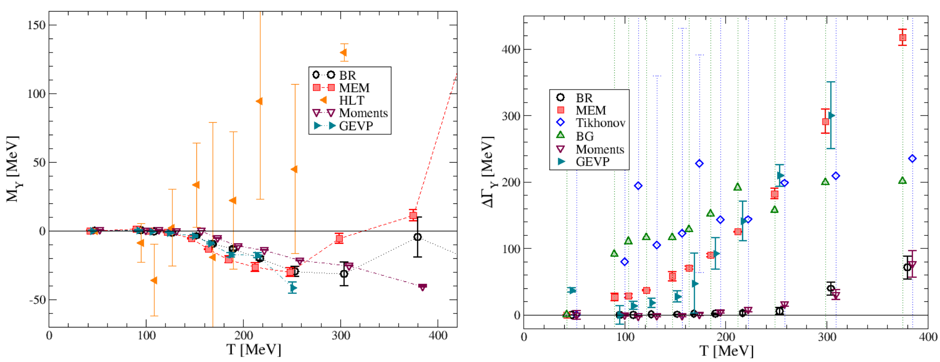

Fig. 1. The thermal mass shift (left) and width (right) of the $\Upsilon(1S)$ using different methods. The results show the difference between the thermal and equivalent zero-temperature results, see the text for details.

We see that the linear methods have much larger uncertainties than the others, which is not surprising as they are not designed to identify narrow peaks in spectral functions (although they become exact in the continuous-time limit). The other methods all find a small but significant negative mass shift of up to 40 MeV. All methods show a thermal width that increases with temperature, but they differ in its magnitude, so at present we can only place an upper bound on the width.

4. B mesons

We constructed two-point correlation functions for B mesons by combining NRQCD propagators for the b quark with relativistic propagators for the light anti-quark. The two are combined by tracing the upper two Dirac indices (in the nonrelativistic representation) of the light-(anti-)quark propagator with the full NRQCD propagator and the appropriate spin matrices to produce pseudoscalar and vector states.

The light-quark propagator is computed with anti-periodic boundary conditions in the temporal extent, while the NRQCD heavy-quark propagator satisfies an initial condition problem. This results in the light-quark propagator containing both forward and backward propagation and the NRQCD heavy-quark propagator only forward propagation. To ensure we only considering the forward propagating light anti-quark, we restrict our analysis to $\tau \leq N_\tau/2$.

Figure 2 (left) shows the mass of the B (pseudoscalar) and B^* (vector) mesons determined from the standard exponential fits, as a function of temperature, from the Gen2 ensembles. The masses are higher than the experimental values since we are using heavier-than-physical light quarks. We also show the results from the $T = 0$ ensembles with truncated correlators as described in Section 3. Comparing the two, we see clear evidence of a negative thermal mass shift for $T \gtrsim 140\,\text{MeV}$, well below the chiral transition temperature T_c.

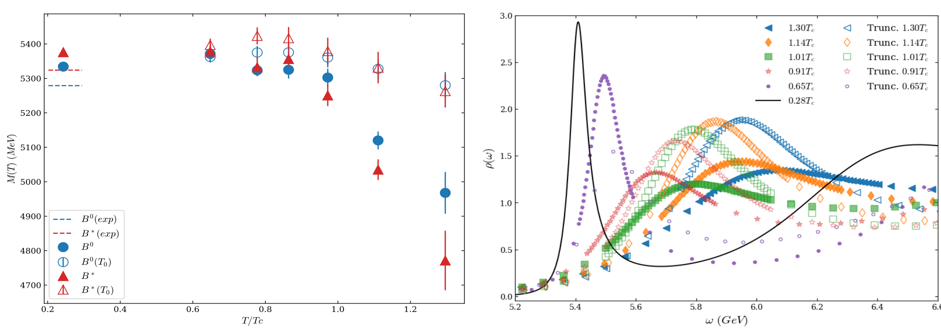

Fig. 2. Left: The mass of the B and B^* mesons as a function of temperature, compared to the masses extracted from $T = 0$ correlators truncated to the same temporal extent. Right: B meson spectral functions from the BR method (solid lines), together with spectral functions obtained from truncated $T = 0$ correlators (dashed lines).

We have also carried out a spectral reconstruction using the BR method. The results for the B meson are shown in Fig. 2 (right). We find that the ground-state peak disappears around T_c, whereas the spectral function from the equivalent truncated $T = 0$ correlator still exhibits a clear peak, suggesting that there is no bound state above T_c.

The analysis for the Gen2L ensembles is in progress, and preliminary results support the conclusions presented above.

5. Static-quark potential

The static-quark potential on the Gen2L ensemble has been computed from Coulomb-gauge Wilson line correlators, which were computed with the SIMULATeQCD code [13]. The potential has been determined from the Wilson line correlators using two methods: BR spectral function reconstruction, and the "UV subtraction" method presented in Ref. [14]. In the latter method, the assumption is that the spectral function consists of a ground-state peak plus a temperature-independent "UV" part. The UV contribution to the correlator can be easily isolated at zero temperature and subtracted from the correlator at all temperatures. The resulting ground-state peak is then modelled by a Gaussian, which corresponds to an effective mass as a function of τ describing a straight line, with the slope giving the imaginary part of the potential and the intercept at $\tau = 0$ giving the real part.

We have also modified this method by assuming that the spectrum may contain a temperature-dependent first excited state in addition to the ground state. A sample of the results, using both assumptions, is shown in Fig. 3

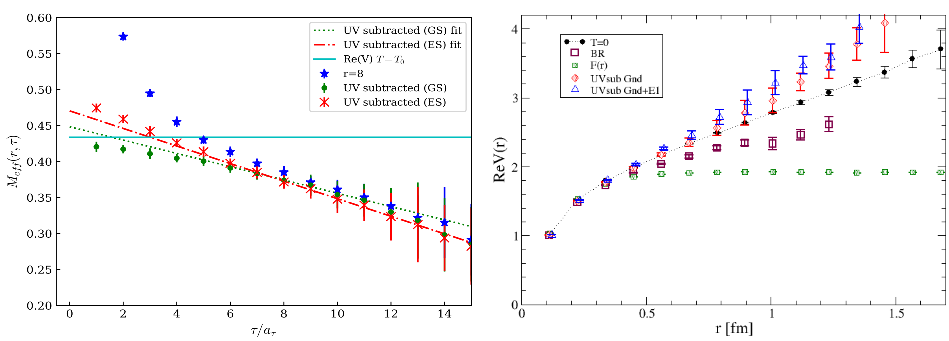

Fig. 3. The static-quark potential from the Gen2L ensemble at $T/T_c = 1.5\,(N_\tau = 24)$. Left: Effective energies of the Wilson line correlator at $r/a_s = 8$ from $T = 0$, 1-state (GS) and 2-state (ES+GS) UV subtracted correlators, together with fits to the UV-subtracted correlators, assuming a single Gaussian form. Right: The static-quark potential from the BR and UV-subtraction methods, compared with the $T = 0$ potential and the free energy.

(left panel). Here, we see that at $T \approx 1.5\,T_c$ and $r \approx 0.9$ fm, the UV-subtracted effective mass does not describe a straight line (invalidating the assumption of a single Gaussian), and a fit to a straight line yields a value for $\mathrm{Re}\,V$ which is larger than the $T = 0$ value. Including the excited state yields a value which lies even higher. The resulting values for $\mathrm{Re}\,V$ are shown in Fig. 3 (right), together with the $T = 0$ potential, the static quark–anti-quark free energy, and the results from the BR method.

Whereas the UV-subtraction method applied to our data suggests anti-screening at high temperature, the BR results indicate screening, and are inconsistent with both the $T = 0$ potential and the free energy. We are currently investigating modifications of the UV subtraction method to better model the shape of the ground-state peak, which should be a skewed Lorentzian rather than a Gaussian.

This work is supported by STFC grant ST/X000648/1. R.H.D. acknowledges support from a Maynooth University John and Pat Hume award and a Research Ireland scholarship. G.A. is supported by a Royal Society Leverhulme Trust Senior Research Fellowship. R.B. acknowledges support from a Science Foundation Ireland Frontiers for the Future Project award with grant number SFI-21/FFP-P/10186. S.K. is supported by the National Research Foundation of Korea through the grant, NRF-2008-000458. A.R. acknowledges support from Korea University via project K2605081 "Ab-initio lattice simulations of the real-time dynamics of non-relativistic fermions". We acknowledge the use of computing resources from the Irish Centre for High-End Computing (ICHEC) and Supercomputing Wales. This work used the DiRAC Data Intensive service (DIaL2 & DIaL) at the University of Leicester, managed by the University of Leicester Research Computing Service on behalf of the STFC DiRAC HPC Facility (www.dirac.ac.uk), the DiRAC Extreme Scaling service (Tursa) at the University of Edinburgh, managed by the Edinburgh Parallel Computing Centre on behalf of DiRAC, and PRACE resources at CINECA (Marconi).

REFERENCES

[1] A. Andronic *et al.*, *Eur. Phys. J. A* **60**, 88 (2024).

[2] R.G. Edwards, B. Joó, H.-W. Lin, *Phys. Rev. D* **78**, 054501 (2008).

[3] Hadron Spectrum Collaboration (H.-W. Lin *et al.*), *Phys. Rev. D* **79**, 034502 (2009).

[4] G. Aarts *et al.*, *J. High Energy Phys.* **2015**, 186 (2015).

[5] G. Aarts *et al.*, *Phys. Rev. D* **105**, 034504 (2022).

[6] G. Aarts *et al.*, arXiv:2209.14681 [hep-lat].

[7] G. Aarts *et al.*, *J. High Energy Phys.* **2014**, 97 (2014).
[8] R.H. D'Arcy *et al.*, *PoS* **(LATTICE2024)**, 203 (2025).
[9] R. Bignell *et al.*, *PoS* **(LATTICE2024)**, 202 (2025).
[10] A. Smecca *et al.*, *PoS* **(LATTICE2024)**, 197 (2025).
[11] Y. Burnier, A. Rothkopf, *Phys. Rev. Lett.* **111**, 182003 (2013).
[12] J.-I. Skullerud *et al.*, *PoS* **(QCHSC24)**, 160 (2025).
[13] HotQCD Collaboration (L. Mazur *et al.*), *Comput. Phys. Commun.* **300**, 109164 (2024).
[14] HotQCD Collaboration (A. Bazavov *et al.*), *Phys. Rev. D* **109**, 074504 (2024).